Synthetic Analogs of the Active Sites of Iron–Sulfur Proteins. VII.[1] Ligand Substitution Reactions of the Tetranuclear Clusters $[Fe_4S_4(SR)_4]^{2-}$ and the Structure of $[(CH_3)_4N]_2[Fe_4S_4(SC_6H_5)_4]$

L. Que, Jr.,[2] M. A. Bobrik,[2] James A. Ibers,[3] and R. H. Holm*[2]

Contribution from the Departments of Chemistry, Massachusetts Institute of Technology, Cambridge, Massachusetts 02139, and Northwestern University, Evanston, Illinois 60201. *Received February 2, 1974*

Abstract: The tetramer $[Fe_4S_4(S\text{-}t\text{-}Bu)_4]^{2-}$ in acetonitrile solution at ambient temperature undergoes facile ligand substitution reactions with thiols R′SH yielding $[Fe_4S_4(S\text{-}t\text{-}Bu)_{4-n}(SR')_n]^{2-}$. The reactions have been monitored by electronic spectral and pmr studies of equilibrium solutions. In the cases of R′ = *p*-$C_6H_4NMe_2$ and *p*-tolyl the n = 1–4 species have been detected in the contact-shifted methyl pmr spectra and equilibrium constants for ligand exchange between two such species approach statistical values. The following ligand substitution series was established: MeC(O)SH ~ *p*-$XC_6H_4SH \gtrsim$ Ac-L-Cys-NHMe $\gtrsim$ *p*-YC_6H_4SH > $PhCH_2SH$ > $HOCH_2CH_2SH$ > EtSH ≫ *p*-MeC_6H_4OH (X = H, NO_2, Me; Y = NMe_2, NMe_3^+). Substitution tendencies roughly parallel aqueous acidities, at least to $pK_a \gtrsim 6.5$, and aryl thiols effect full substitution at (R′SH)/(tetramer) mole ratios of 4.5–4.9. The structure of a representative aryl-substituted tetramer, $(Me_4N)_2[Fe_4S_4(SPh)_4]$, has been determined from 2844 independent reflections collected by counter methods. The red-black crystals are orthorhombic, space group D_2^4-$P2_12_12_1$, with a = 11.704 (11), b = 23.944 (16), and c = 14.876 (10) Å and a calculated density of 1.492 g/cm³ for four formula units in the unit cell. The structure consists of discrete cations and anions. The Fe_4S_4* core, as that of $[Fe_4S_4(SCH_2Ph)_4]^{2-}$, has effective D_{2d} symmetry. The principal difference between the structures of the two tetramers occurs in the detailed geometry of the Fe_4 portion, which in $[Fe_4S_4(SPh)_4]^{2-}$ more closely approaches T_d symmetry with an average Fe···Fe distance of 2.736 Å. The bonded Fe–S* distances occur as sets of four (2.267 (5) Å) and eight (2.296 (4) Å), giving an average of 2.286 Å. The average terminal Fe–S distance is 2.263 Å. Comparison of the structures of the two tetramers does not provide any clear indication that $[Fe_4S_4(SPh)_4]^{2-}$ is inherently the more stable. The positions of the ligand substitution equilibria are concluded to be dominated by the acid–base characteristics of *tert*-butylthiolate and R′SH. The utility of the ligand substitution reactions in synthesis is illustrated by the preparation and isolation of salts of $[Fe_4S_4(SPh)_4]^{2-}$ and $[Fe_4S_4(SePh)_4]^{2-}$ by reaction of $[Fe_4S_4(S\text{-}t\text{-}Bu)_4]^{2-}$ with benzenethiol and diphenyl diselenide, respectively, in acetonitrile solution.

Recent investigations in these laboratories have resulted in the synthesis of the tetranuclear complexes $[Fe_4S_4(SR)_4]^{2-}$ [4,5] and demonstration that these species are close structural[5] and electronic[1,4,6,7] representations of the active sites of oxidized 4-Fe and 8-Fe ferredoxin proteins and the reduced "high-potential" *Chromatium* protein.[8–10] The structure of $[Fe_4S_4(SCH_2Ph)_4]^{2-}$ [4,5] reveals the cubane-type stereochemistry (**1**) with D_{2d} symmetry. The equivalence of all metal sites apparent in the crystalline state at ambient temperature has been shown to extend to this and other tetrameric dianions by measurements using spectroscopic techniques capable of sensing widely different lifetimes of electronic states.[11] Consequently,

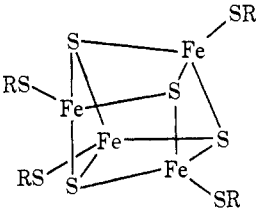

1

$[Fe_4S_4(SR)_4]^{2-}$ complexes are regarded as fully delocalized rather than trapped valence [2Fe(II) + 2Fe(III)] species.

In addition to their structural and electronic features, the reactivity properties of $[Fe_4S_4(SR)_4]^{2-}$ complexes have been investigated. Results available at present indicate that the dianions undergo two types of reactions. The first is electron transfer affording the redox series $[Fe_4S_4(SR)_4]^z$. Voltammetric evidence indicates existence of the members z = 4−, 3−, 2−, and 1− with the 3−/2− interconversion being reversible in most cases.[1,7] The second type of reaction is suggested by the tetrahedral coordination of iron in **1** and the paramagnetic (antiferromagnetic[4]) nature of the Fe_4S_4 core. These two factors should promote lability of the thiolate groups bonded to iron. Previous examples of reactions at tetrahedral M(II, III) centers have been mainly confined to intramolecular

(1) Part VI: B. V. DePamphilis, B. A. Averill, T. Herskovitz, L. Que, Jr., and R. H. Holm, *J. Amer. Chem. Soc.*, **96**, 4159 (1974).
(2) Massachusetts Institute of Technology.
(3) Northwestern University.
(4) T. Herskovitz, B. A. Averill, R. H. Holm, J. A. Ibers, W. D. Phillips, and J. F. Weiher, *Proc. Nat. Acad. Sci. U. S.*, **69**, 2437 (1972).
(5) B. A. Averill, T. Herskovitz, R. H. Holm, and J. A. Ibers, *J. Amer. Chem. Soc.*, **95**, 3523 (1973).
(6) R. H. Holm, W. D. Phillips, B. A. Averill, J. J. Mayerle, and T. Herskovitz, *J. Amer. Chem. Soc.*, **96**, 2109 (1974).
(7) R. B. Frankel, T. Herskovitz, B. A. Averill, R. H. Holm, P. J. Krusic, and W. D. Phillips, *Biochem. Biophys. Res. Commun.*, in press.
(8) C. W. Carter, Jr., J. Kraut, S. T. Freer, R. A. Alden, L. C. Sieker, E. Adman, and L. H. Jensen, *Proc. Nat. Acad. Sci. U. S.*, **69**, 3526 (1972).
(9) E. T. Adman, L. C. Sieker, and L. H. Jensen, *J. Biol. Chem.*, **248**, 3987 (1973).
(10) For reviews *cf.* J. C. M. Tsibris and R. W. Woody, *Coord. Chem. Rev.*, **5**, 417 (1970); G. Palmer and H. Brintzinger in "Electron and Coupled Energy Transfer in Biological Systems," Vol. 1, Part B, T. E. King and M. Klingenberg, Ed., Marcel Dekker, New York, N. Y., 1972, Chapter 9; W. H. Orme-Johnson, *Annu. Rev. Biochem.*, **42**, 159 (1973).
(11) R. H. Holm, B. A. Averill, T. Herskovitz, R. B. Frankel, H. B. Gray, O. Siiman, and F. J. Grunthaner, *J. Amer. Chem. Soc.*, **96**, 2644 (1974).

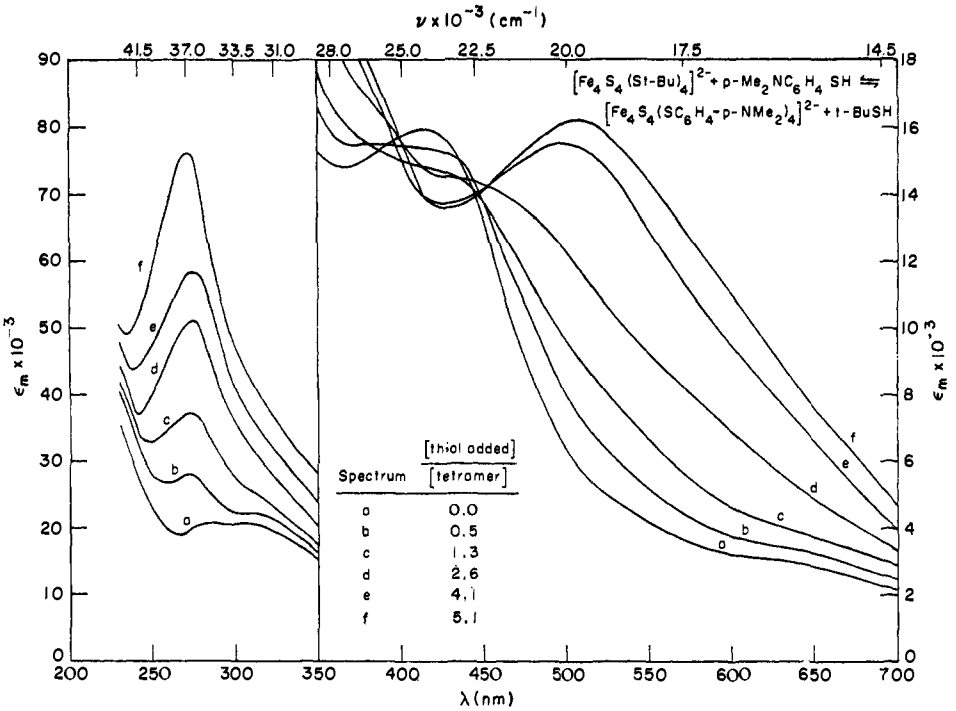

Figure 1. Electronic spectral changes caused by addition of varying amounts of *p*-dimethylaminobenzenethiol to an acetonitrile solution of $(Ph_4As)_2[Fe_4S_4(S\text{-}t\text{-}Bu)_4]$ at ambient temperature.

stereochemical isomerization processes of certain M(II) systems.[12,13] Substitution and ligand exchange reactions have been much less extensively examined,[14] a situation presumably resulting from the known or assumed high degree of lability of ligands bonded to such centers. The only detailed study of reactions of these types with tetrahedral iron complexes has been a pmr determination of phosphine exchange kinetics involving several dihalobis(triarylphosphine)iron(II) species.[15] Recently we have shown that $[Fe_4S_4(SR)_4]^{2-}$ complexes (R = alkyl) in nonaqueous media undergo facile substitution reactions with certain thiols and that *p*-tolylthiol produces the fully substituted tetramer upon reaction with $[Fe_4S_4(S\text{-}t\text{-}Bu)_4]^{2-}$ in only slightly more than the stoichiometric (4/1) ratio.[16] Similar ligand substitution reactions are described in more detail in this report, and it is shown that solution equilibria at ambient temperature favor formation of aryl- *vs.* alkyl-substituted tetramers. Factors affecting the equilibria are considered, and the structure of the typical aryl-substituted tetramer $[Fe_4S_4(SPh)_4]^{2-}$, determined as its tetramethylammonium salt, is presented and compared with that of $[Fe_4S_4(SCH_2Ph)_4]^{2-}$.

Experimental Section

Preparation of Compounds.[17] **$(Ph_4As)_2[Fe_4S_4(S\text{-}t\text{-}Bu)_4]$.** This compound, obtained by the usual tetramer synthesis,[5] was prepared in order to obtain a more soluble salt of the previously reported dianion.[5,6] It was obtained as red-brown crystals, mp 210–212° dec, and was not analyzed but was identified by pmr[6] (Figure 1) and electronic[1] spectra.

Synthesis by Ligand Substitution. (a) $(Ph_4As)_4[Fe_4S_4(SPh)_4]$. To a solution of 0.385 g (0.261 mmol) of $(Ph_4As)_2[Fe_4S_4(S\text{-}t\text{-}Bu)_4]$ in 10 ml of acetonitrile was added 140 μl (~1.4 mmol) of benzenethiol. The solution color changed to reddish brown. Addition of 150 ml of 4:1 v/v methanol–water afforded, after filtering, washing with methanol–water, and drying for 10 hr, 0.355 g (87%) of product as small black crystals. Final purification was carried out by recrystallization from acetonitrile–methanol–water, yielding 0.223 g (55%), mp 191–192° (product from direct synthesis,[5] mp 191–193°).

(b) $(Ph_4As)_2[Fe_4S_4(SePh_4)]$. To a solution of 0.680 g (0.461 mmol) of $(Ph_4As)_2[Fe_4S_4(S\text{-}t\text{-}Bu)_4]$ in 35 ml of acetonitrile was added 0.72 g (2.3 mmol) of diphenyl diselenide dissolved in ~100 ml of acetonitrile. The solution was stirred for 20 hr at room temperature during which time the color changed to purplish red. The volume was reduced until crystals began to precipitate, at which point the solution was warmed to 40° to redissolve the solid. Addition of methanol and slow cooling to −10° afforded 0.64 g (80%) of reddish black crystals. Final purification was achieved by recrystallization from acetonitrile–methanol: mp 163–165°; λ_{max} (ε, acetonitrile) 468 nm (16,100). *Anal.* Calcd for $C_{72}H_{60}As_2Fe_4S_4Se_4$: C, 49.63; H, 3.47; As, 8.60; Fe, 12.82; S, 7.36; Se, 18.12. Found: C, 49.48; H, 3.52; As, 8.44; Fe, 12.82; S, 7.22; Se, 17.97.

Ligand Substitution Reactions. *p*-Nitrobenzenethiol,[5] *N*-acetyl-L-cysteine-*N*-methylamide,[1] *p*-dimethylaminobenzenethiol,[18] and *p*-trimethylammoniumbenzenethiol hexafluorophosphate[1] were prepared or purified as described elsewhere. Other thiols were the best commercial grades available. The reactions, which involve the replacement SR/SR′ by reaction of $[Fe_4S_4(SR)_4]^{2-}$ with the thiol R′SH (text, eq 1), were followed by pmr and electronic spectral measurements of equilibrium solutions with exclusion of oxygen. Pmr spectra were obtained at ~30° on a Varian HA-100 or an Hitachi-Perkin-Elmer R20B 60-MHz spectrometer, which was operated in the Fourier transform mode. In typical experiments the spectral changes resulting from the addition of varying amounts of R′SH to 0.02 *M* solutions of $(Ph_4As)_2[Fe_4S_4(S\text{-}t\text{-}Bu)_4]$ were monitored. Chemical shifts were determined relative to TMS

(12) R. H. Holm and M. J. O'Connor, *Progr. Inorg. Chem.*, **14**, 241 (1971).
(13) S. S. Eaton and R. H. Holm, *Inorg. Chem.*, **10**, 1446 (1971).
(14) F. Basolo and R. G. Pearson, "Mechanisms of Inorganic Reactions," 2nd ed, Wiley, New York, N. Y., 1967, pp 435–445; A. Peloso, *Coord. Chem. Rev.*, **10**, 123 (1973).
(15) L. H. Pignolet, D. Forster, and W. D. Horrocks, Jr., *Inorg. Chem.*, **7**, 828 (1968).
(16) M. Bobrik, L. Que, Jr., and R. H. Holm, *J. Amer. Chem. Soc.*, **96**, 285 (1974).
(17) All manipulations were carried out under a nitrogen atmosphere. Melting points were determined in evacuated tubes and are uncorrected.
(18) G. Chuchani and A. Frohlich, *J. Chem. Soc. B*, 1417 (1971).

internal standard. As previously,[6] shifts downfield of TMS are taken as negative.

Spectrophotometric data were recorded on a Cary Model 14 instrument. Stock solutions of *ca.* 3.5×10^{-3} *M* $(Ph_4As)_2[Fe_4S_4(S\text{-}t\text{-}Bu)_4]$ and 0.1–0.7 *M* R′SH were prepared under nitrogen in pure degassed acetonitrile. An aliquot of the tetramer solution was introduced into a quartz titration cell with a 0.1-mm path length, and spectra were recorded after addition by microsyringe of aliquots of thiol solution. The data for the ligand replacement series in Table II were obtained by the addition of 4.0 equiv of thiol followed by successive additions of 0.1 equiv of thiol. Substitution was considered complete when addition of thiol produced no further spectral changes associated with the tetramer species. Spectra of a series of $[Fe_4S_4(SR)_4]^{2-}$ complexes have been reported elsewhere.[1] Solution volume changes were negligible owing to the high concentrations of thiol solutions. Limiting spectra are in excellent agreement with the spectra of isolated salts of $[Fe_4S_4(SR)_4]^{2-}$ determined separately in acetonitrile. In all cases equilibrium appeared to be established within several minutes or less. Pmr and spectrophotometric measurements were made no sooner than 15 min after solution preparation.

Crystal Data for $(Me_4N)_2[Fe_4S_4(SPh)_4]$. Air-sensitive red-black crystals of this compound, prepared and purified by the usual procedure,[5] were transferred under dry nitrogen to predried capillaries. Weissenberg and precession photographs with both Mo Kα and Cu Kα radiation indicated that the compound crystallizes in space group D_2^4-$P2_12_12_1$ of the orthorhombic system. Unit cell dimensions were obtained from the centering of 12 reflections on a FACS-1 automatic diffractometer using techniques previously described.[19] The 12 reflections had 2θ values in the range 19–24° (Mo Kα_1). Based on λ(Mo Kα_1) of 0.70930 Å the dimensions are a = 11.704 (11), b = 23.944 (16), and c = 14.876 (10) Å at 21°. The calculated density for four formula units in the unit cell is 1.492 g/cm³. No experimental density was obtained owing to the air sensitivity of the crystals. With four formula units in the cell no crystallographic symmetry is imposed on the anion or the cations.

Data Collection and Reduction. The crystal selected for data collection was needle-like in habit with approximate overall dimensions 0.8 mm along the needle axis by about 0.15 × 0.15 mm in cross section. The needle axis is [100]. The crystal used had 14 faces consisting of those from the forms {100}, {011}, {010}, and {101} and in addition the faces $(1\bar{2}\bar{2})$ and (111). The calculated volume of the crystal is 0.0178 mm³.

The crystal was mounted on a Picker FACS-I diffractometer with the [100] axis misset from the spindle axis by about 8°. Data were collected using Mo Kα radiation that had been monochromatized from the (002) face of a highly mosaic graphite crystal. The takeoff angle used was 2.15° and the counter to crystal distance was 32 cm. The counter aperture was 4 mm wide by 5.5 mm high. No overlapping reflections were found as judged by the scan tracings. In the θ–2θ collection mode the scan speed was 2° in 2θ/min from 1.0° in 2θ below the Kα_1 peak to 1.0° in 2θ above the Kα_2 peak. Background counting times were 10 sec for $2\theta < 34°$, 20 sec for $34° < 2\theta < 43.5°$, and 40 sec for $43.5 < 2\theta < 50°$. Past 50° in 2θ only about 10% of the reflections were above background in trial scans and so data collection was terminated. A total of 4148 unique reflections was collected. Of these 2844 had $F^2 \geq 3\sigma(F^2)$ and were used in the refinement. Six standard reflections were collected every 100 reflections; variations were within counting statistics, and hence there was no evidence for crystal decomposition. Data were processed in the usual way[19,20] with p = 0.03. Transmission factors ranged from 0.723 to 0.814 using a linear absorption coefficient for Mo Kα radiation of 17.74 cm^{-1}.

Structure Solution and Refinement. The direct methods approach, based on 195 normalized structure factors, yielded the correct positions of the four Fe and eight S atoms of the anion.[21] The other nonhydrogen atoms were found in a subsequent difference Fourier synthesis.

Refinement of the structure was by full-matrix least-squares methods. The procedures and sources of atomic scattering factors have been given previously.[5] In all refinements the phenyl rings were constrained to D_{6h} symmetry with the C–C distance taken at 1.392 Å and were allotted individual, variable isotropic thermal parameters. The course of the refinement, as indicated by values of R and R_w in parentheses, was as follows: isotropic refinement of 12 heavy atoms (0.216, 0.300); complete isotropic refinement of all nonhydrogen atoms (0.074, 0.081); anisotropic refinement of all nonhydrogen atoms—first cycle (0.050, 0.055); final anisotropic refinement including fixed contributions for the hydrogen atoms (0.041, 0.043).

The phenyl hydrogen atoms were idealized to a C–H distance of 0.95 Å and assigned B values 1 Å² greater than the carbon atoms to which they are attached. Methyl hydrogen atoms of the cations were found in difference Fourier syntheses and were idealized for tetrahedral geometry and a C–H distance of 0.95 Å and were assigned B values of 10 Å².

In the final refinement of 247 variables based on 2844 observations, the error in an observation of unit weight is 1.44 electrons. A final difference Fourier synthesis showed a maximum density of 0.4 (1) e/Å³, approximately 15% of the height of a carbon atoms in previous difference maps. Analysis of $\Sigma w(|F_o| - |F_c|)^2$ as a function of Miller indices, $|F_o|$, and setting angles revealed no particular trends. Calculation of $|F_c|$ for those reflections for which $I < 3\sigma(I)$ revealed only 7 out of 1304 reflections having $|F_o^2 - F_c|^2 > 3\sigma(F_o^2)$. These reflections are not included in the table[22] which gives values of $10|F_o|$ and $10|F_c|$ (in electrons) for the 2844 reflections used in the refinement.

Listed in Table IV are the final parameters together with the standard deviations of these parameters as estimated from the inverse matrix. Listed in Table VII are the positional parameters for the ring carbon atoms that may be derived from Table IV. Calculated positions of the hydrogen atoms are given in Table VI,[22] and the root-mean-square amplitudes of vibration that may be derived from the data of Table IV are set out in Table V. The directions of the principal axes of vibration are discernible from Figures 5 and 6.

Results and Discussion

Ligand Substitution Reactions. In this investigation reactions have been sought which allow substitution of thiolate ligands in $[Fe_4S_4(SR)_4]^{2-}$ under conditions sufficiently mild to avoid any significant decomposition of the Fe_4S_4 core. As reported recently,[16] this objective can be achieved by reaction of free thiols R′SH with a tetramer in a process represented generally by eq 1. This reaction has been monitored by

$$[Fe_4S_4(SR)_4]^{2-} + n\text{R}'\text{SH} \rightleftharpoons [Fe_4S_4(SR)_{4-n}(SR')_n]^{2-} + n\text{RSH} \quad (1)$$

electronic and pmr spectroscopy. In nearly all cases $[Fe_4S_4(S\text{-}t\text{-}Bu)_4]^{2-}$, in the form of its adequately soluble tetraphenylarsonium salt, was employed as the initial tetramer. It was selected on the basis of preliminary experiments which indicated that it was equally or more prone to substitution reactions than other tetramers with R = alkyl. In addition, the signals of coordinated t-butylthiolate and free t-BuSH are readily identified and are not obscured by other resonances. These experiments also revealed that the equilibrium position of reaction 1 lies strongly to the right when R′ = aryl.

The system $[Fe_4S_4(S\text{-}t\text{-}Bu)_4]^{2-}$–$p$-$Me_2NC_6H_4SH$ in acetonitrile provides a representative case of ligand exchange involving an aromatic thiol. The electronic spectral changes observed upon the addition of the

(19) P. W. R. Corfield, R. J. Doedens, and J. A. Ibers, *Inorg. Chem.*, **6**, 197 (1967).

(20) R. J. Doedens and J. A. Ibers, *Inorg. Chem.*, **6**, 204 (1967).

(21) In addition to local programs for the CDC 6400 used in this work, local versions of the following programs were employed: MULTAN, direct methods program of Main, Germain, and Woolfson; FORDAP, Fourier program of Zalkin; AGNOST, absorption program (employing the Gaussian integration logic of Coppens, Leiserowitz, and Rabinovich); ORFFE, function and error program of Busing and Levy; ORTEP, thermal ellopsoid plotting program of Johnson; TMA, thermal analysis program of Dunitz and White (employing the Schomaker–Trueblood algorithms). Our least-squares program, NUCLS, in its nongroup form, closely resembles the ORFLS program of Busing and Levy.

(22) See paragraph at the end of this article for supplementary material available.

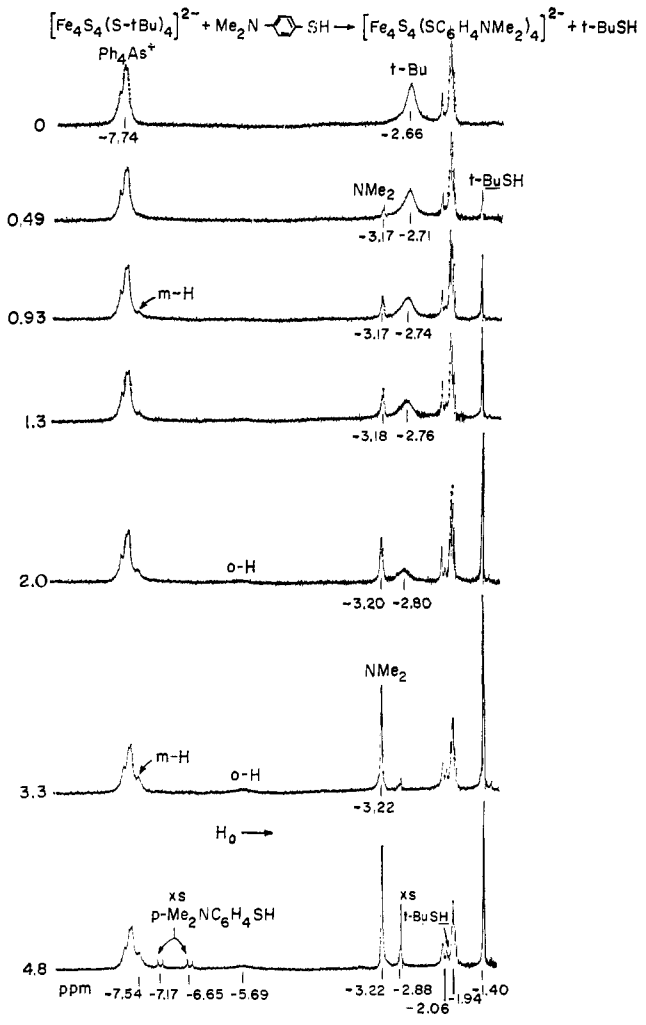

Figure 2. Pmr spectral changes (100 MHz) caused by the addition of varying amounts of *p*-dimethylaminobenzenethiol to a CD_3CN solution of $(Ph_4As)_2[Fe_4S_4(S\text{-}t\text{-}Bu)_4]$ at ambient temperature. Numerical values refer to mole ratios of added thiol to original tetramer. Chemical shifts are downfield of TMS internal reference.

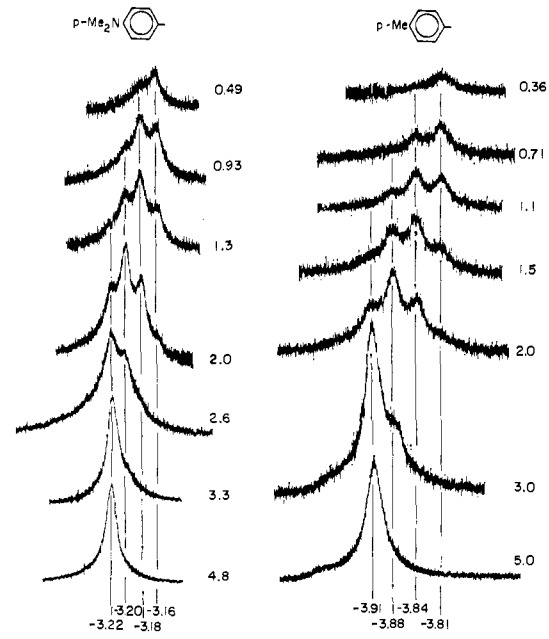

Figure 3. Methyl pmr spectral changes (100 MHz) caused by the addition of varying amounts of *p*-dimethylaminobenzenethiol (left) and *p*-tolylthiol (right) to a CD_3CN solution of $(Ph_4As)_2[Fe_4S_4(S\text{-}t\text{-}Bu)_4]$ at ambient temperature. Numerical values refer to mole ratios of added thiol to original tetramer. Chemical shifts are downfield of TMS internal reference. Signals in consecutive downfield order arise from the $n = 1, 2, 3, 4$ species (text, eq 1) in both cases.

thiol to a solution of the tetramer are shown in Figure 1. The spectrum of the initial tetramer (curve a, λ_{max} 413 nm, ϵ 16,900) is altered upon the addition of 0.5 equiv of thiol. Introduction of more thiol produces a progressive low-energy shift in this spectral region until, at a (R'SH)/(tetramer) mole ratio of 4.9/1 (*vide infra*), the limiting spectrum, represented by curve f, is reached. The corresponding pmr results are presented in Figure 2. Recent work has shown that all $[Fe_4S_4(SR)_4]^{2-}$ species exhibit isotropically shifted pmr spectra in which the displacements of R signals from their normal diamagnetic positions in free thiols arise predominantly from contact interactions.[6] The spectrum of $[Fe_4S_4(S\text{-}t\text{-}Bu)_4]^{2-}$ consists of a single broad resonance at −2.66 ppm. Addition of *p*-dimethylaminobenzenethiol results in the emergence of three signals downfield of the *t*-Bu resonance, which can only be assigned to coordinated thiolate, and a feature at −1.40 ppm from *t*-BuSH. The intensities of all of these signals increase as aromatic thiol is added. At the ratio (R'SH)/(tetramer) = 4.8/1 free R'SH signals are clearly evident (ring-H −6.65, −7.17 ppm; CH_3 −2.88 ppm), and the coordinated *t*-Bu peak has disappeared. Integration of the *t*-BuSH *vs.* the Ph_4As^+ + *m*-H signals indicates that at this ratio full substitution has been attained. Chemical shifts of the resonances arising from *o*-H, *m*-H, and NMe_2 are identical with those of $[Fe_4S_4(SC_6H_4\text{-}p\text{-}NMe_2)_4]^{2-}$ measured separately. Similar spectrophotometric and pmr results for the system $[Fe_4S_4(S\text{-}t\text{-}Bu)_4]^{2-}$–*p*-$MeC_6H_4SH$ are given elsewhere.[16]

The course of ligand substitution reactions has been examined in more detail by expansion of the isotropically shifted methyl signals in the systems $[Fe_4S_4(S\text{-}t\text{-}Bu)_4]^{2-}$–*p*-$Me_2NC_6H_4SH$ and –*p*-MeC_6H_4SH. Spectra obtained at various (R'SH)/(tetramer) ratios are shown in Figure 3. For the system containing *p*-dimethylaminobenzenethiol two signals are evident at a ratio of 0.49/1 with that at higher field (−3.16 ppm) being more intense. Addition of more thiol causes diminution of this signal, growth and decay of signals at −3.18 and −3.20 ppm, and growth of the feature at −3.22 ppm. The latter is the only signal remaining at the 4.8/1 ratio, at which point full substitution has occurred. These spectral changes indicate that the multiplicity of resonances arises from mixed ligand tetramers. With reference to eq 1 the following signal assignments are made: −3.16, $n = 1$; −3.18, $n = 2$; −3.20, $n = 3$; −3.22 ppm, $n = 4$. Similar conclusions follow from inspection of the spectra obtained for the *p*-tolylthiol system. Spectra of coordinated *t*-Bu groups in these and other systems were not sufficiently resolved to permit detection of mixed ligand tetramers. However, the progressive downfield shift of the *t*-Bu signal in the above two systems (*cf.* Figure 2 and Figure 2 of ref 16) presumably arises from changes in spin density distribution effected by substitution of an aliphatic by an aromatic thiolate ligand. The pmr results additionally indicate that the equilibria do not favor full substitution at the expense of mixed ligand

Table I. Ratios of Equilibrium Constants for *p*-tolS–*t*-BuS Exchange in CD_3CN Solution at ~30°

System	Ratio	$K_1' = K_1/K_2$	$K_2' = K_2/K_3$	$K_3' = K_3/K_4$
p-tolSH–	0.36[a]	1.8[c]		
$[Fe_4S_4(S\text{-}t\text{-}Bu)_4]^{2-}$	0.71[a]	2.3		
	1.09[a]	2.1	1.9	
	1.51[a]		2.0	1.7
$[Fe_4S_4(S\text{-}p\text{-}tol)_4]^{2-}$–	0.97[b]	1.8	1.7	
$[Fe_4S_4(S\text{-}t\text{-}Bu)_4]^{2-}$	1.94[b]		1.8	2.0
	2.09[b]		1.9	1.9
	2.62[b]		1.6	2.0
Mean		2.0 ± 0.3	1.7 ± 0.3	1.9 ± 0.3
Statistical value		2.67	2.24	2.67

[a] Mole ratio of thiol to original tetramer. [b] Mole ratio of *p*-tolS coordinated ligands to total tetramer. [c] Estimated error ±15%.

Table II. Ligand Replacement Series for $[Fe_4S_4(SR)_4]^{2-}$ in Acetonitrile Solution

R	R′SH	Fraction sub tetramer[a]	Equiv R′SH for complete subn[b]	pK_a(R′SH)[c]
t-Bu	CH_3COSH	0.98	4.6	3.20[d]
t-Bu	*p*-$O_2NC_6H_4SH$	0.97	4.5	4.50[d]
t-Bu	C_6H_5SH	0.96	4.5	6.43[d]
t-Bu	*p*-$CH_3C_6H_4SH$	0.98	4.5	6.52[e]
t-Bu	Ac-L-Cys-NHMe	0.93	*i*	*g*
t-Bu	*p*-$Me_2NC_6H_4SH$	0.90	4.9	7.41[f]
t-Bu	*p*-$Me_3\overset{+}{N}C_6H_4SH$	*h*	4.9	*g*
t-Bu	$PhCH_2SH$	0.85	*i*	9.4[e]
t-Bu	$HOCH_2CH_2SH$	0.78	*i*	9.61[d]
t-Bu	CH_3CH_2SH	0.59	*i*	10.61[e]
t-Bu	*p*-$CH_3C_6H_4OH$	0.17		10.70[f]
Et	*p*-$CH_3C_6H_4SH$		4.6	6.52[e]
	t-BuSH			11.1–11.2

[a] Equiv of *t*-BuSH released/4 equiv R′SH added, determined by pmr at ~30°, estimated error ±3%. [b] Spectral values at 25°, estimated error ±0.1 equiv. [c] Data refer to aqueous solution unless otherwise noted. [d] W. P. Jencks and K. Salvesen, *J. Amer. Chem. Soc.*, **93**, 4433 (1971). [e] J. P. Danehy and K. N. Parameswaran, *J. Chem. Eng. Data*, **13**, 386 (1968). [f] 20% aqueous ethanol, ref 18. [g] Not reported. [h] Thiol salt insufficiently soluble. [i] Insufficient spectral differences for determination.

Table III. Isotropic Proton Shifts

Complex	Shift (ppm) Ortho	Meta	Para
$[Fe_4S_4(SPh)_4]^{2-}$ [a,b]	+1.56	−0.89	+2.09
$[Fe_4S_4(SePh)_4]^{2-}$ [a,c,d]	+0.92	−0.82	+1.52
$[Fe_4S_4(SC_6H_4\text{-}p\text{-}NMe_2)_4]^{2-}$ [c,e,f]	+1.48	−0.89	−0.34

[a] DMSO-d_6 solution. [b] 22°, data from ref 6. [c] ~30°. [d] Diamagnetic reference PhSeSePh. [e] CD_3CN solution. [f] Diamagnetic reference free thiol.

formation. In the (R′SH)/(tetramer) range of *ca.* 0.4–4.0, at least two species are clearly detectable, with the n = 1, 2, and 3 tetramers observable at the 2/1 ratio in both systems.

The individual equilibrium constants K_n (eq 2) for

$$K_n = \frac{[Fe_4S_4(S\text{-}t\text{-}Bu)_{4-(n+1)}(SR')_{n+1}][t\text{-BuSH}]}{[Fe_4S_4(S\text{-}t\text{-}Bu)_{4-n}(SR')_n][R'SH]} \quad (2)$$

ligand substitution reactions involving aromatic thiols were not obtained because the concentration of added thiol could not be measured. At (R′SH)/(tetramer) ratios where mixed ligand species can be detected, substitution of *tert*-butylthiolate appears to be essentially quantitative from the integrated intensities of *t*-Bu signals. However, ratios of these constants (K_{n+1}/K_n) can be approximated by signal integration and also are the equilibrium constants for thiolate exchange between two tetramers. These reactions can be described by the choice of three independent equilibrium constants (eq 3). In this case $K_1' = K_1/K_2$, $K_2' = K_2/K_3$,

$$[Fe_4S_4(S\text{-}t\text{-}Bu)_4]^{2-} + [Fe_4S_4(S\text{-}t\text{-}Bu)_2(SR')_2]^{2-} \overset{K_1'}{\rightleftharpoons} 2[Fe_4S_4(S\text{-}t\text{-}Bu)_3(SR')]^{2-}$$

$$[Fe_4S_4(S\text{-}t\text{-}Bu)_3(SR')]^{2-} + [Fe_4S_4(S\text{-}t\text{-}Bu)(SR')_3]^{2-} \overset{K_2'}{\rightleftharpoons} 2[Fe_4S_4(S\text{-}t\text{-}Bu)_2(SR')_2]^{2-} \quad (3)$$

$$[Fe_4S_4(S\text{-}t\text{-}Bu)_2(SR')_2]^{2-} + [Fe_4S_4(SR')_4]^{2-} \overset{K_3'}{\rightleftharpoons} 2[Fe_4S_4(S\text{-}t\text{-}Bu)(SR')_3]^{2-}$$

and $K_3' = K_3/K_4$. The results for two different systems are summarized in Table I. The relative concentrations of the various species were determined by signal integration and that of $[Fe_4S_4(S\text{-}t\text{-}Bu)_4]^{2-}$ was obtained by difference. Only the *t*-BuS–*p*-tolS exchange was studied because the methyl signals of differently substituted tetramers are somewhat better resolved than those in systems containing the *p*-dimethylaminobenzenethiolate ligand. Because the total span of chemical shifts is only 0.1 ppm (Figure 3), the data are not highly precise due to signal overlap. However, their precision is sufficient to show that the derived equilibrium constants approach statistical values.

Ligand Substitution Series. An important aspect of ligand substitution reactions is a knowledge of the relative tendencies of added thiols R′SH to replace coordinated thiolate in a given tetramer. In the absence of the equilibrium constants K_n or the overall equilibrium constants for full substitution, the desired information may be obtained in several ways. In pmr experiments 4.0 equiv of thiol was added to 1.0 equiv of a *ca.* 0.02 *M* solution of $(Ph_4As)_2[Fe_4S_4(S\text{-}t\text{-}Bu)_4]$ in CD_3CN at ~30°. The amount of *t*-BuSH released was determined by integration *vs.* the cation resonance and when divided by the 4 equiv of added thiol gives the fraction of tetramer substituted. In cases where the electronic spectra of $[Fe_4S_4(S\text{-}t\text{-}Bu)_4]^{2-}$ and $[Fe_4S_4(SR')_4]^{2-}$ are sufficiently different, 4.0 equiv of R′SH was added to 1.0 equiv of a *ca.* 3.5×10^{-3} *M* acetonitrile solution of the former and the resulting solution was titrated with thiol until a limiting spectrum was reached. This method is useful when R′SH is an aromatic thiol due to the large spectral differences[1] between aliphatic- (λ_{max} 415–425 nm) and aromatic-substituted tetramers (λ_{max} 450–510 nm). The results are set out in Table II. The most important conclusion is that, within the series of thiols employed, the substitution tendencies of R′SH show a correlation with aqueous acidity in the range $10.6 \leq pK_a \sim 6.5$. Consequently, aromatic thiols substitute more effectively than do aliphatic thiols. The methods utilized do not differentiate among the substitution tendencies of thiols with $pK_a \lesssim 6.5$. The only thiol carboxylic acid examined, thioacetic acid, exhibits a degree of substitution qualitatively consistent with its relatively high acidity. According to spectral results, *p*-tri-

Table IV. Final Parameters for $[NMe_4]_2[Fe_4S_4(SPh)_4]$

Atom	x	y	z	β_{11}[a]	β_{22}	β_{33}	β_{12}	β_{13}	β_{23}
Fe(1)	0.18143 (12)[b]	0.32134 (6)	0.38918 (9)	0.00763 (12)	0.00218 (3)	0.00532 (7)	0.00035 (5)	0.00073 (8)	0.00021 (4)
Fe(2)	0.09834 (11)	0.35208 (5)	0.22479 (9)	0.00701 (10)	0.00162 (2)	0.00575 (7)	0.00020 (4)	−0.00056 (8)	−0.00005 (4)
Fe(3)	0.32662 (10)	0.36383 (5)	0.26278 (8)	0.00667 (10)	0.00175 (2)	0.00482 (6)	−0.00025 (4)	−0.00035 (8)	0.00001 (3)
Fe(4)	0.23532 (10)	0.26010 (5)	0.23906 (8)	0.00721 (11)	0.00149 (2)	0.00558 (7)	0.00027 (4)	0.00025 (8)	0.00012 (4)
S(1)	0.24744 (21)	0.33033 (9)	0.13439 (14)	0.00886 (21)	0.00167 (4)	0.00441 (11)	0.00001 (9)	−0.00035 (14)	0.00001 (6)
S(2)	0.35586 (20)	0.28730 (10)	0.35301 (16)	0.00749 (20)	0.00228 (5)	0.00526 (13)	0.00048 (9)	−0.00009 (13)	0.00050 (7)
S(3)	0.05916 (21)	0.27026 (10)	0.29929 (17)	0.00720 (20)	0.00188 (5)	0.00737 (15)	−0.00039 (8)	0.00060 (14)	0.00025 (7)
S(4)	0.17947 (23)	0.40992 (9)	0.33070 (16)	0.00982 (23)	0.00178 (5)	0.00600 (13)	0.00033 (9)	−0.00014 (17)	−0.00062 (7)
S(5)	0.11172 (23)	0.30783 (13)	0.52895 (18)	0.00921 (24)	0.00352 (7)	0.00638 (15)	−0.00074 (11)	0.00202 (17)	0.00040 (9)
S(6)	−0.06375 (21)	0.37958 (11)	0.15472 (20)	0.00708 (21)	0.00250 (6)	0.00971 (19)	−0.00036 (9)	−0.00216 (17)	0.00104 (9)
S(7)	0.49776 (23)	0.40489 (11)	0.23403 (17)	0.00865 (21)	0.00339 (6)	0.00614 (15)	−0.00187 (11)	−0.00163 (16)	0.00094 (9)
S(8)	0.28096 (22)	0.18578 (9)	0.15271 (17)	0.01130 (25)	0.00158 (4)	0.00540 (13)	0.00051 (9)	0.00108 (15)	0.00015 (6)
N(1)	−0.37170 (67)	0.23132 (33)	0.10767 (50)	0.01058 (80)	0.00255 (18)	0.00507 (44)	−0.00086 (32)	0.00149 (51)	−0.00032 (25)
C(1)	−0.25071 (88)	0.24940 (56)	0.09655 (81)	0.01060 (95)	0.00681 (42)	0.01199 (83)	−0.00491 (54)	0.00176 (81)	0.00001 (50)
C(2)	−0.37787 (99)	0.17065 (41)	0.09495 (71)	0.0165 (13)	0.00217 (22)	0.00837 (70)	−0.00019 (45)	0.00297 (82)	−0.00032 (33)
C(3)	−0.4125 (10)	0.24506 (48)	0.19955 (61)	0.0173 (13)	0.00479 (34)	0.00655 (51)	−0.00160 (55)	0.00143 (68)	−0.00225 (34)
C(4)	−0.4414 (11)	0.26055 (50)	0.04085 (67)	0.0175 (15)	0.00402 (31)	0.00906 (71)	0.00010 (58)	−0.00183 (84)	0.00124 (41)
N(2)	−0.25985 (76)	0.36469 (37)	0.44422 (53)	0.01090 (84)	0.00233 (20)	0.00630 (48)	0.00060 (38)	−0.00145 (56)	0.00014 (26)
C(5)	−0.2524 (14)	0.32926 (47)	0.36381 (78)	0.0314 (21)	0.00364 (29)	0.00843 (75)	0.00139 (71)	0.0005 (12)	−0.00157 (40)
C(6)	−0.3787 (10)	0.36941 (65)	0.46940 (97)	0.0149 (12)	0.00759 (52)	0.0152 (11)	0.00382 (68)	0.00262 (98)	−0.00124 (66)
C(7)	−0.1988 (13)	0.33864 (54)	0.51705 (83)	0.0373 (23)	0.00474 (38)	0.01479 (85)	0.00452 (79)	−0.0166 (12)	0.00042 (49)
C(8)	−0.2230 (15)	0.41759 (74)	0.4223 (11)	0.0455 (24)	0.00324 (54)	0.0166 (13)	−0.0053 (10)	0.0033 (17)	0.00023 (76)

Ring[c]	x_c	y_c	z_c	δ	ϵ	η
R(1)	0.25566 (43)	0.37818 (21)	0.66860 (31)	0.8871 (47)	−3.0226 (47)	0.7903 (41)
R(2)	0.02201 (36)	0.47008 (17)	0.01528 (28)	−1.0587 (52)	−2.4056 (36)	−2.0149 (54)
R(3)	0.50356 (37)	0.44784 (16)	0.03309 (26)	−1.8884 (38)	3.0684 (37)	−1.9216 (36)
R(4)	0.24718 (36)	0.07739 (16)	0.27037 (22)	−1.6229 (38)	−2.9950 (41)	0.5455 (32)

[a] The form of the anisotropic thermal ellipsoid is $\exp[-(\beta_{11}h^2 + \beta_{22}k^2 + \beta_{33}l^2 + 2\beta_{12}hk + 2\beta_{13}hl + 2\beta_{23}kl)]$. [b] Here and in succeeding tables estimated standard deviations are parenthesized. [c] These group parameters have been defined previously. See, for example, S. J. La Placa and J. A. Ibers, *Acta Crystallogr.*, **18**, 511 (1965).

Table V. Root-Mean-Square Amplitudes of Vibration (Å)

Atom	Min	Int	Max	Atom	Min	Int	Max
Fe(1)	0.221 (2)	0.241 (2)	0.264 (2)	S(8)	0.210 (3)	0.238 (3)	0.290 (3)
Fe(2)	0.211 (2)	0.222 (2)	0.257 (2)	N(1)	0.223 (11)	0.252 (10)	0.302 (11)
Fe(3)	0.209 (2)	0.228 (2)	0.236 (2)	C(1)	0.200 (13)	0.369 (13)	0.479 (14)
Fe(4)	0.204 (2)	0.226 (2)	0.252 (2)	C(2)	0.249 (13)	0.277 (14)	0.365 (14)
S(1)	0.220 (3)	0.221 (3)	0.250 (3)	C(3)	0.232 (12)	0.327 (13)	0.414 (14)
S(2)	0.217 (3)	0.237 (3)	0.271 (3)	C(4)	0.284 (12)	0.348 (16)	0.372 (15)
S(3)	0.212 (3)	0.241 (3)	0.290 (3)	N(2)	0.235 (12)	0.267 (11)	0.296 (12)
S(4)	0.213 (3)	0.259 (3)	0.274 (3)	C(5)	0.263 (14)	0.357 (15)	0.470 (16)
S(5)	0.216 (4)	0.293 (4)	0.324 (3)	C(6)	0.270 (13)	0.421 (16)	0.494 (17)
S(6)	0.209 (3)	0.255 (3)	0.349 (3)	C(7)	0.196 (13)	0.386 (16)	0.613 (17)
S(7)	0.212 (3)	0.248 (3)	0.348 (3)	C(8)	0.263 (31)	0.428 (18)	0.586 (15)

Table VII. Derived Parameters for the Ring Carbon Atoms

Atom	x	y	z	B (Å²)
R(1)C(1)	0.19502 (58)	0.34957 (27)	0.60258 (38)	4.9 (2)
R(1)C(2)	0.30466 (61)	0.33228 (27)	0.62596 (50)	6.9 (3)
R(1)C(3)	0.36530 (48)	0.36089 (36)	0.69199 (56)	9.1 (4)
R(1)C(4)	0.31631 (70)	0.40679 (33)	0.73462 (45)	9.4 (4)
R(1)C(5)	0.20667 (72)	0.42408 (25)	0.71124 (49)	8.5 (3)
R(1)C(6)	0.14603 (47)	0.39547 (29)	0.64521 (49)	5.9 (2)
R(2)C(1)	−0.01580 (51)	0.43103 (22)	0.07790 (37)	4.2 (2)
R(2)C(2)	−0.06346 (45)	0.43226 (24)	−0.00784 (43)	5.4 (2)
R(2)C(3)	−0.02565 (57)	0.47130 (29)	−0.07046 (31)	6.9 (3)
R(2)C(4)	0.05983 (58)	0.50912 (25)	−0.04735 (38)	6.3 (3)
R(2)C(5)	0.10749 (47)	0.50789 (23)	0.03839 (43)	5.5 (2)
R(2)C(6)	0.06968 (52)	0.46885 (26)	0.10102 (31)	5.1 (2)
R(3)C(1)	0.49855 (52)	0.42761 (23)	0.12073 (28)	4.1 (2)
R(3)C(2)	0.40343 (41)	0.45341 (26)	0.08283 (40)	5.1 (2)
R(3)C(3)	0.40844 (49)	0.47364 (26)	−0.00481 (42)	6.2 (2)
R(3)C(4)	0.50857 (63)	0.46807 (27)	−0.05455 (29)	6.8 (3)
R(3)C(5)	0.60369 (47)	0.44227 (27)	−0.01666 (40)	6.3 (2)
R(3)C(6)	0.59868 (42)	0.42204 (24)	0.07098 (41)	4.9 (2)
R(4)C(1)	0.26148 (51)	0.12679 (18)	0.22234 (32)	3.8 (2)
R(4)C(2)	0.15253 (41)	0.10469 (25)	0.23451 (40)	5.7 (2)
R(4)C(3)	0.13823 (43)	0.05529 (27)	0.28254 (46)	7.1 (3)
R(4)C(4)	0.23288 (60)	0.02799 (20)	0.31840 (36)	6.2 (2)
R(4)C(5)	0.34183 (48)	0.05010 (24)	0.30623 (40)	5.9 (2)
R(4)C(6)	0.35612 (38)	0.09950 (25)	0.25820 (42)	5.2 (2)

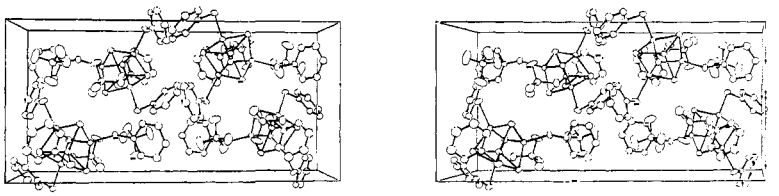

Figure 4. A stereoscopic view of the unit cell of $(Me_4N)_2[Fe_4S_4(SPh)_4]$. Hydrogen atoms have been omitted for the sake of clarity. The atoms depicted have been drawn with vibrational ellipsoids at the 20% probability level. In the drawing the origin is at the upper right, with the y axis running from right to left, the x axis from top to bottom, and the z axis into the paper.

methylammoniumbenzenethiol and *p*-dimethylaminobenzenethiol are equally effective in substitution, despite the higher acidity of the former anticipated from correlation of substituent constants with pK_a.[18] Pmr studies in DMSO-d_6, described elsewhere,[1] suggest that the thiol cation may be involved in ion pairing as well as substitution. Lastly, *p*-cresol, the only nonsulfur ligand tested, shows a much smaller affinity for substitution than either the much more acidic *p*-tolylthiol or the equally acidic ethanethiol. This result indicates that acidity alone is not a reliable index for substitution affinity and implies that oxygen acids will in general be less effective than thiols in substitution reactions. Factors affecting the position of equilibrium 1 are further considered in a following section.

Synthesis by Ligand Substitution. The facile substitution reactions described above offer a simple synthetic route to variously substituted tetramers, especially those which rank near the top of the ligand replacement series in Table II. Reaction of $[Fe_4S_4(S\text{-}t\text{-}Bu)_4]^{2-}$ with *ca.* 5.5 equiv of benzenethiol in acetonitrile at room temperature afforded $[Fe_4S_4(SPh)_4]^{2-}$ in good but nonoptimized yield (55%) after purification as its tetraphenylarsonium salt. While this tetramer has been synthesized by the direct method described earlier,[5] the ligand substitution reactions have the advantages of short reaction times (<15 min) and less complicated reaction mixtures. Salts of the tetramer $[Fe_4S_4(S\text{-}t\text{-}Bu)_4]^{2-}$ are readily prepared and purified in large quantities and serve as precursors for the synthesis of new tetramers. In addition, removal of the volatile *t*-BuSH (bp 64°) shifts the equilibria (1) in favor of the desired tetramer. Advantage of these factors and the relatively high position of acetyl-L-cysteine-*N*-methylamide in the substitution series has been taken in the preparation of $[Fe_4S_4(S\text{-}Cys(Ac)NHMe)_4]^{2-}$, which has proved difficult to obtain by the direct method. Other experiments to be reported subsequently have shown that tetrameric complexes containing cysteinyl peptides can be prepared from $[Fe_4S_4(S\text{-}t\text{-}Bu)_4]^{2-}$ and the peptide in the thiol form.[23]

In a variation of the substitution reactions utilizing thiols, the first selenium-containing synthetic tetramer has been obtained in 80% yield by reaction 4. This

$$[Fe_4S_4(S\text{-}t\text{-}Bu)_4]^{2-} + 2PhSeSePh \longrightarrow [Fe_4S_4(SePh)_4]^{2-} + 2t\text{-}BuSSBu\text{-}t \quad (4)$$

reaction is in effect a redox process and is substantially slower than substitution by thiols. It can presumably be extended to the synthesis of other thio and seleno tetramers, and its principal advantage in the present case is the avoidance in the reaction mixture of the objectionable benzeneselenol.

Pmr Shifts of Aryl Tetramers. A previous study has demonstrated that the signs and, to a semiquantitative extent, the relative magnitudes of proton isotropic shifts in $[Fe_4S_4(SR)_4]^{2-}$, R = Ph or substituted phenyl, are consistent with dominant contact inter-

(23) L. Que, Jr., J. R. Anglin, M. A. Bobrik, A. Davison, and R. H. Holm, results to be submitted for publication.

actions arising from ligand → metal spin delocalization.[6] Data for $[Fe_4S_4(SPh)_4]^{2-}$ and two new tetramers obtained in this work are given in Table III. The pattern of shifts for $[Fe_4S_4(SePh)_4]^{2-}$ is similar to that of its sulfur analog, indicating the same delocalization mechanism. This comment also applies to $[Fe_4S_4(SC_6H_4\text{-}p\text{-}NMe_2)_4]^{2-}$, whose shifts may be rationalized in terms of structures **2–4**. The near coplanarity

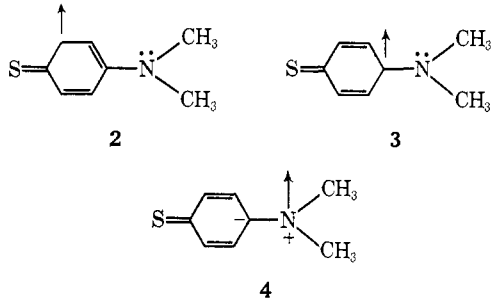

2 **3**

4

of phenyl and dimethylamino groups found in 4-dimethylaminodiphenyl sulfide[24] should apply here, facilitating spin delocalization on nitrogen. As in the case of $[Fe_4S_4(S\text{-}p\text{-}tol)_4]^{2-}$,[6] a direct contact interaction with the methyl protons *via* hyperconjugation can occur, leading to the observed negative shifts.[25] These interactions are undoubtedly principally responsible for the methyl chemical shift differences among the variously substituted tetramers (Figure 3) which permit detection of these species.

As the data of Table II reveal, ligand substitution reactions of $[Fe_4S_4(S\text{-}t\text{-}Bu)_4]^{2-}$ strongly favor the formation of an aryl- *vs.* alkyl-substituted tetramer. In order to investigate the factors which might influence the relative equilibrium positions of these reactions, the structure of $[Fe_4S_4(SPh)_4]^{2-}$ as its tetramethylammonium salt has been determined.

Description of the Structure of $(Me_4N)_2[Fe_4S_4(SPh)_4]$. The structure consists of discrete cations and anions. Shown in Figure 4 is a stereoview of the contents of the unit cell. A stereoview of the complete anion is given in Figure 5. Least-squares planes for the anion are listed in Table VIII. Selected distances and angles for the ions are presented in Table IX. The principal dimensions of the Fe_4S_8 portion of the anion together with the atom labeling scheme are given in Figure 6. The ions are well separated, the closest calculated distance of approach being 2.20 Å between R(1)H(3) and R(4)H(2) of the phenyl rings of adjacent anions.

The tetramethylammonium ions have their expected tetrahedral geometry with no evidence of disorder, and their structure is apparent from Figure 4. The atoms of the cation, particularly C(5) through C(8), exhibit a high degree of thermal motion, as may be ascertained from Figure 4 and Table IV. The apparent mean N–C distance is 1.455 (12) Å, an unexpectedly short value which is undoubtedly the result of thermal motion. When a correction for librational motion of the assumed rigid bodies is applied, the mean distance increases to 1.534 Å.

(24) C. Panattoni, G. Bandoli, D. A. Clemente, A. Dondoni, and A. Mangini, *J. Cryst. Mol. Struct.*, 3, 65 (1973).

(25) A similar isotropic shift pattern has been observed for bis(*N*,*N*'-di-*p*-dimethylaminophenylaminotroponeiminato)nickel(II), one member of an extensive series of related complexes in which the main delocalization mechanism is ligand → metal spin transfer: D. R. Eaton, A. D. Josey, W. D. Phillips, and R. E. Benson, *J. Chem. Phys.*, 37, 347 (1962).

Table VIII. Best Weighted Least-Squares Planes for the Anion

Plane no.	$Ax + By + Cz = D$ (orthorhombic coordinates)							$Ax + By + Cz = D$ (orthorhombic coordinates)			
	A	*B*	*C*	*D*	Plane no.	*A*	*B*	*C*	*D*
1	4.507	21.884	1.907	8.584	7	9.949	−7.333	−6.374	−3.094
2	4.117	−6.626	13.302	2.428	8	0.266	20.271	−7.910	5.455
3	6.839	−19.343	1.154	−4.513	9	6.166	10.968	10.650	6.792
4	7.291	9.080	−10.178	1.636	10	0.359	20.201	−7.973	3.362
5	2.745	−12.767	−12.091	−6.934	11	6.249	10.822	10.630	8.823
6	11.393	2.424	3.056	4.039	12	9.926	−7.403	−6.401	−1.071

Atom	Deviations (Å) from plane no.											
	1	2	3	4	5	6	7	8	9	10	11	12
Fe(1)	0.008 (1)		−0.013 (1)		−0.004 (1)	0.062 (1)				0.091 (1)	−0.075 (1)	
Fe(2)	−0.007 (1)			−0.010 (1)	−0.009 (1)		0.057 (1)	−0.070 (1)	0.070 (1)			−0.062 (1)
Fe(3)		0.002 (1)	0.012 (1)		0.008 (1)			−0.071 (1)			−0.051 (1)	−0.049 (1)
Fe(4)		−0.002 (1)		0.009 (1)		0.003 (1)			0.058 (1)	0.070 (1)		
S(1)	0.017 (2)		−0.030 (2)			−0.009 (2)		0.244 (2)	−0.212 (3)			0.222 (2)
S(2)	−0.019 (2)			−0.025 (2)	−0.026 (2)					−0.246 (2)	0.263 (2)	0.217 (2)
S(3)		0.006 (3)	0.035 (3)		0.027 (3)		−0.207 (2)		−0.275 (3)	−0.268 (2)		
S(4)		−0.006 (3)		0.029 (3)		0.010 (3)	−0.235 (3)	0.287 (2)			0.250 (2)	

Table IX. Selected Distances (Å) and Angles (deg)

N–C		Fe–S		Fe···Fe		S*–S*–S*	
N(1)–C(1)	1.49 (1)	Fe(1)–S(5)	2.257 (3)	Fe(1)–Fe(2)	2.733 (2)	S(4)–S(1)–S(3)	61.32 (8)
N(1)–C(2)	1.47 (1)	Fe(2)–S(6)	2.263 (3)	Fe(3)–Fe(4)	2.727 (2)	S(4)–S(2)–S(3)	61.16 (8)
N(1)–C(3)	1.48 (1)	Fe(3)–S(7)	2.272 (3)	Mean	2.730	S(1)–S(3)–S(2)	60.88 (8)
N(1)–C(4)	1.46 (1)	Fe(4)–S(8)	2.259 (3)	Fe(1)–Fe(3)	2.731 (2)	S(1)–S(4)–S(2)	60.96 (7)
N(2)–C(5)	1.47 (1)	Mean	2.263 (3)	Fe(1)–Fe(4)	2.745 (2)	Mean	61.08
N(2)–C(6)	1.45 (1)	Fe···S*		Fe(2)–Fe(3)	2.745 (3)	S(4)–S(1)–S(2)	59.92 (8)
N(2)–C(7)	1.44 (1)	Fe(1)–S(1)	3.874 (4)	Fe(2)–Fe(4)	2.733 (2)	S(3)–S(1)–S(2)	59.41 (8)
N(2)–C(8)	1.38 (2)	Fe(2)–S(2)	3.890 (3)	Mean	2.739 (4)	S(4)–S(2)–S(1)	59.17 (6)
Mean	1.455 (12)[a]	Fe(3)–S(3)	3.888 (4)	Mean (of 6)	2.736 (3)	S(3)–S(2)–S(1)	59.71 (7)
C–N–C		Fe(4)–S(4)	3.893 (3)	S–Fe–S*		S(1)–S(3)–S(4)	59.06 (7)
C(1)–N(1)–C(2)	108.7 (9)	Mean	3.886 (4)	S(5)–Fe(1)–S(2)	119.6 (1)	S(2)–S(3)–S(4)	59.66 (7)
C(1)–N(1)–C(3)	110.1 (8)	S*···S*		S(5)–Fe(1)–S(3)	103.5 (1)	S(1)–S(4)–S(3)	59.62 (7)
C(1)–N(1)–C(4)	108.4 (9)	S(1)–S(2)	3.640 (4)	S(5)–Fe(1)–S(4)	118.6 (1)	S(2)–S(4)–S(3)	59.18 (8)
C(2)–N(1)–C(3)	108.8 (8)	S(3)–S(4)	3.659 (4)	S(6)–Fe(2)–S(1)	116.1 (1)	Mean	59.47
C(2)–N(1)–C(4)	111.0 (9)	Mean	3.650	S(6)–Fe(2)–S(3)	107.6 (1)	S*–Fe–S*	
C(3)–N(1)–C(4)	109.9 (8)	S(1)–S(3)	3.597 (4)	S(6)–Fe(2)–S(4)	119.1 (1)	S(2)–Fe(1)–S(3)	103.3 (1)
C(5)–N(2)–C(6)	108.2 (11)	S(1)–S(4)	3.577 (4)	S(7)–Fe(3)–S(1)	110.8 (1)	S(2)–Fe(1)–S(4)	104.6 (1)
C(5)–N(2)–C(7)	109.5 (9)	S(2)–S(3)	3.587 (5)	S(7)–Fe(3)–S(2)	108.9 (1)	S(3)–Fe(1)–S(4)	105.3 (1)
C(5)–N(2)–C(8)	108.7 (11)	S(2)–S(4)	3.605 (4)	S(7)–Fe(3)–S(4)	135.7 (1)	S(1)–Fe(2)–S(3)	104.1 (1)
C(6)–N(2)–C(7)	108.5 (11)	Mean	3.592 (6)	S(8)–Fe(4)–S(1)	100.2 (1)	S(1)–Fe(2)–S(4)	103.1 (1)
C(6)–N(2)–C(8)	106.9 (12)	Fe–Fe–Fe		S(8)–Fe(4)–S(2)	119.8 (1)	S(3)–Fe(2)–S(4)	105.4 (1)
C(7)–N(2)–C(8)	114.9 (11)	Fe(4)–Fe(1)–Fe(3)	59.73 (5)	S(8)–Fe(4)–S(3)	121.7 (1)	S(1)–Fe(3)–S(4)	103.6 (1)
Mean	109.5	Fe(4)–Fe(2)–Fe(3)	59.71 (6)	Mean	115.1	S(2)–Fe(3)–S(4)	103.9 (1)
Fe–S*–Fe		Fe(1)–Fe(3)–Fe(2)	59.87 (6)	Fe–S*		S(1)–Fe(3)–S(2)	105.7 (1)
Fe(2)–S(1)–Fe(4)	73.63 (8)	Fe(1)–Fe(4)–Fe(2)	59.86 (5)	Fe(1)–S(2)	2.263 (3)	S(1)–Fe(4)–S(3)	104.3 (1)
Fe(2)–S(1)–Fe(3)	74.55 (9)	Mean	59.79	Fe(2)–S(1)	2.264 (3)	S(2)–Fe(4)–S(3)	103.7 (1)
Fe(4)–S(1)–Fe(3)	73.35 (9)	Fe(4)–Fe(1)–Fe(2)	59.85 (6)	Fe(3)–S(4)	2.281 (3)	S(1)–Fe(4)–S(2)	104.7 (1)
Fe(1)–S(2)–Fe(3)	73.58 (8)	Fe(3)–Fe(1)–Fe(2)	60.33 (7)	Fe(4)–S(3)	2.261 (3)	Mean	104.3
Fe(1)–S(2)–Fe(4)	73.97 (9)	Fe(4)–Fe(2)–Fe(1)	60.30 (5)	Mean	2.267 (5)	S–C (ring)	
Fe(3)–S(2)–Fe(4)	72.77 (9)	Fe(3)–Fe(2)–Fe(1)	59.80 (5)	Fe(1)–S(3)	2.309 (3)	S(5)–R(1)C(1)	1.775 (7)
Fe(4)–S(3)–Fe(2)	73.66 (8)	Fe(2)–Fe(3)–Fe(4)	59.91 (4)	Fe(1)–S(4)	2.293 (3)	S(6)–R(2)C(1)	1.772 (6)
Fe(4)–S(3)–Fe(1)	73.82 (10)	Fe(1)–Fe(3)–Fe(4)	60.39 (5)	Fe(2)–S(3)	2.297 (3)	S(7)–R(3)C(1)	1.771 (5)
Fe(2)–S(3)–Fe(1)	72.78 (9)	Fe(2)–Fe(4)–Fe(3)	60.38 (7)	Fe(2)–S(4)	2.303 (3)	S(8)–R(4)C(1)	1.766 (5)
Fe(3)–S(4)–Fe(1)	73.32 (9)	Fe(1)–Fe(4)–Fe(3)	59.88 (5)	Fe(3)–S(1)	2.269 (3)	Mean	1.771 (2)
Fe(3)–S(4)–Fe(2)	73.58 (9)	Mean	60.11	Fe(3)–S(2)	2.297 (3)	Fe–S–C (ring)	
Fe(1)–S(4)–Fe(2)	72.98 (9)	Mean (of 12)	60.00	Fe(4)–S(1)	2.296 (3)	Fe(1)–S(5)–R(1)C(1)	106.8 (2)
Mean	73.50			Fe(4)–S(2)	2.300 (3)	Fe(2)–S(6)–R(2)C(1)	103.5 (2)
				Mean	2.296 (4)	Fe(3)–S(7)–R(3)C(1)	108.5 (2)
						Fe(4)–S(8)–R(4)C(1)	105.4 (2)
						Mean	106.1

[a] If given, the value in parentheses is the standard deviation of the mean as estimated from the agreement among the averaged values. The estimated standard deviation of the mean is not given for any angular quantity, as the variations exceed those expected from a sample taken from the same population.

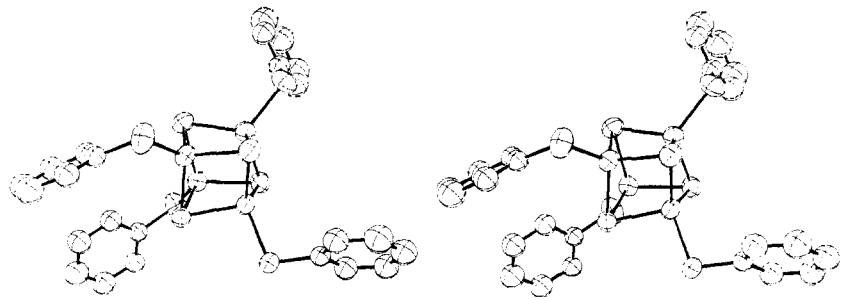

Figure 5. A stereoscopic view of the $[Fe_4S_4(SPh)_4]^{2-}$ ion, complete except for hydrogen atoms. The 50% probability ellipsoids are shown.

As may be seen from Figures 4–6 $[Fe_4S_4(SPh)_4]^{2-}$, as $[Fe_4S_4(SCH_2Ph)_4]^{2-}$, [5] possesses the cubane-type stereochemistry **1** and hence also serves as a structural representation of the active sites of the proteins mentioned at the outset. Relevant considerations of the anion structure follow those given in more detail for the benzylthiolate tetramer.[5] For ease in structural comparison the orientation of the anion and the atom labeling scheme in Figure 6 correspond to that for $[Fe_4S_4(SCH_2Ph)_4]^{2-}$ (*cf.* Figure 2 of ref 5). A comparison of the mean values of selected structural parameters for the two anions is presented in Table X. The only significant difference between the two structures occurs in the detailed geometry of the Fe_4S_4* core, which is closer to T_d symmetry in $[Fe_4S_4(SPh)_4]^{2-}$. Based on a previous analysis,[5] the values of σ^2 which measure the deviations of the core from a perfect $\bar{4}$ axis along the three principal directions are 18.3, 28.6, and 57.2, compared with the corresponding values of 25.4, 289, and 350 for $[Fe_4S_4(SCH_2Ph)_4]^{2-}$. Examination of the distances and angles in Tables IX and X indicates that, while the S_4* portion of the core deviates from tetrahedral symmetry, the Fe_4 portion in the present structure, as distinct from that in $[Fe_4S_4(SCH_2Ph)_4]^{2-}$, is essentially tetrahedral. The Fe_4S_4* core may still be classified for purposes of convenience as having the symmetry

D_{2d}, but the deviations from T_d symmetry are relatively small. As found for the benzylthiolate tetramer, the six diagonal planes through the core (Table VIII), defined by Fe(n), Fe(m), S*(n), S*(m), where $1 \leq n \leq 3$ and $n < m \leq 4$, are nearly perfect.

The effects of packing forces of the outer portion of the anion are more evident in the present structure. Thus the S–Fe–S* angles range from 100.2 to 135.7°, whereas in $[Fe_4S_4(SCH_2Ph)_4]^{2-}$ these angles vary from 110.4 to 117.3°.[5] Presumably the S–Ph linkage, as opposed to the S–CH_2–Ph linkage, brings about greater distortion of the S–Fe–S* angles because of the bulkiness of the phenyl groups which are directly bonded to sulfur.

Aromatic *vs.* Aliphatic Thiols in Ligand Substitution. The equilibrium positions of the ligand substitution reactions (eq 1) will depend on the relative stabilities (free energies) of initial and final tetramers and thiols. As already pointed out on the basis of the results in Table II, substitution affinities of thiols roughly parallel pK_a values at least down to $pK_a \lesssim 6.5$. However, the aromatic nature of all but one of the more acidic thiols examined raised the possibility that aryl-substituted tetramers might be intrinsically more stable than their alkyl analogs. Insofar as such a stability difference can be inferred from structural results in the solid state, it would appear to be small or negligible from the comparative parameters listed in Table X. In particular, the mean values of all Fe–S*, Fe–S, and Fe···Fe distances in the aryl and alkyl tetramers are identical or only marginally different. There is certainly no indication that the Fe–S bonds external to the core are shorter and thus stronger in $[Fe_4S_4(SPh)_4]^{2-}$. This point is consistent with the roughly statistical values of the equilibrium quotients K_1', K_2', and K_3' (Table I), which are independent of free thiol.

Table X. Comparison of Mean Values of Selected Structural Parameters for $[Fe_4S_4(SCH_2Ph)_4]^{2-}$ and $[Fe_4S_4(SPh)_4]^{2-}$

Distance/angle[a]	$[Fe_4S_4(SCH_2Ph)_4]^{2-}$ [b]	$[Fe_4S_4(SPh)_4]^{2-}$
Fe–S	2.251	2.263
Fe–S*[c]	2.239 (4), 2.310 (8)	2.267 (4), 2.296 (8)
Fe···Fe[d]	2.776 (2), 2.732 (4)	2.730 (2), 2.739 (4)
S–Fe–S*	115.1	114.4
Fe–S*–Fe	73.8	73.5
S*–Fe–S*	104.1	104.3
Fe–Fe–Fe[e]	61.11 (4), 59.46 (8)	59.79 (4), 60.11 (8)

[a] Number of values averaged indicated in parentheses where two distances or angles are given. [b] Et_4N^+ salt; data from ref 5. [c–e] Mean of all values: [c] 2.286 (CH_2Ph, Ph); [d] 2.747 (CH_2Ph), 2.736 (Ph); [e] 60.01 (CH_2Ph), 59.99 (Ph).

We conclude that the positions of the equilibria (1) are dominated by the acid–base characteristics of *t*-butylthiolate and R'SH. All thiols tested which are more acidic than *t*-BuSH (pK_a = 11.1–11.2) cause greater than 50% substitution. That $[Fe_4S_4(SEt)_4]^{2-}$ is as effectively substituted by *p*-tolylthiol as is $[Fe_4S_4(S\text{-}t\text{-}Bu)_4]^{2-}$ (Table II) suggests that any destabilizing steric interactions that may exist in the latter tetramer are not manifested in the position of the substitution equilibria, at least with the more acidic thiols. Consideration of the mechanism of the ligand substitution reaction will be deferred until the completion of stopped-flow kinetic studies.[26]

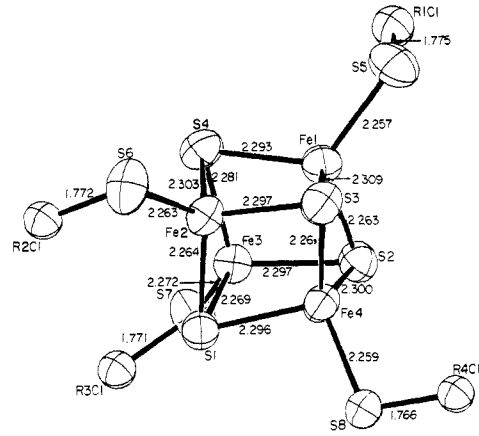

Figure 6. A portion of the $[Fe_4S_4(SPh)_4]^{2-}$ core, showing 50% probability ellipsoids, principal interatomic distances, and the atom labeling scheme.

The ligand substitution reactions described herein enhance both the basic inorganic chemistry and the biological relevance of the Fe–S complexes based on the cubane-type stereochemistry **1**. Among the important consequences of these reactions of $[Fe_4S_4(S\text{-}t\text{-}Bu)_4]^{2-}$ and other alkyl-substituted tetramers are the following: (i) the synthesis of complexes not obtainable or less conveniently obtained by the direct method[5] (*e.g.*, $[Fe_4S_4(S\text{-}Cys(Ac)NHMe)_4]^{2-}$ and other tetramers derived from cysteinyl peptides[23]); (ii) the incorporation of a variety of interesting and useful features such as terminal ligands other than SR (*e.g.*, $[Fe_4S_4(SePh)_4]^{2-}$) and different overall charge (*e.g.*, $[Fe_4S_4(SC_6H_4\text{-}p\text{-}NMe_3)_4]^{2+}$, whose core is isoelectronic with that of $[Fe_4S_4(SR)_4]^{2-}$); and (iii) linkage of two tetramers by reaction with polyfunctional thiols.[16] Other possible reactions include (iv) extrusion of intact Fe–S cluster(s) from holoproteins or enzymes in the form of appropriately substituted tetramer dianions by treatment with thiols (preferably aromatic) in sufficient concentration and (v) reconstitution of the holoprotein from the apoprotein and the preformed Fe–S cluster. Several of these reactions are under active investigation in this laboratory. The only exchange reaction reported thus far for the proteins is the base-catalyzed exchange of iron and sulfide in several clostridial ferredoxins.[27] Exchange of the core components in the synthetic tetramers has not been examined. No indication of decomposition of the Fe_4S_4* core has been observed in any system exhibiting ligand substitution reactions with thiols.

Acknowledgment. We thank B. A. Averill for experimental assistance. This research was supported at the Massachusetts Institute of Technology by Research Grant GM-19256 (National Institutes of Health) and at Northwestern University by Research Grant HL-13157 (National Institutes of Health).

Supplementary Material Available. A tabular listing of structure amplitudes and calculated coordinates of the hydrogen atoms (Table VI) will appear following these pages in the microfilm edi-

(26) G. R. Dukes and R. H. Holm, work in progress.
(27) J.-S. Hong and J. C. Rabinowitz, *J. Biol. Chem.*, **245**, 6582 (1970).

tion of this volume of the journal. Photocopies of the supplementary material from this paper only or microfiche (105 × 148 mm, 24× reduction, negatives) containing all of the supplementary material for the papers in this issue may be obtained from the Journals Department, American Chemical Society, 1155 16th St., N.W., Washington, D. C. 20036. Remit check or money order for $5.00 for photocopy or $2.00 for microfiche, referring to code number JACS-74-4168.

Copper(II) and Zinc(II) Binding of Optically Active Dipeptides[1]

Robert Nakon and Robert J. Angelici* [2]

Contribution from the Department of Chemistry, Iowa State University, Ames, Iowa 50010. *Received January 23, 1974*

Abstract: Equilibrium constants are reported for the protonation and metal ion coordination of L,L ("pure") and D,L ("mixed") diastereomers of the dipeptides Ala-Ala, Ala-Phe, Leu-Leu, and Leu-Tyr. The higher pK_a values of the NH_2 group and the lower pK_a values of the CO_2^- group in the "mixed" as compared to the "pure" diastereomers can be explained by assuming the dipeptides have a predominantly β-conformation under all pH conditions. Solutions of Cu(II) and the dipeptides (HL) form the same general types of complexes previously reported for Gly-Gly: $Cu^{2+} + L^- \rightleftharpoons CuL^+$, K_1; $CuL^+ \rightleftharpoons Cu(H_{-1}L) + H^+$, K_{1a}; $Cu(H_{-1}L) + OH^- \rightleftharpoons Cu(H_{-1}L)(OH)^-$, K_{OH}. The K_1 values for "mixed" dipeptides are larger than for their "pure" diastereomers. This trend is also observed with Zn(II) and can again be rationalized by assuming a β-conformation for the uncomplexed dipeptide anion (L^-). Amide deprotonation of CuL^+ complexes of "pure" dipeptides occurs with K_{1a} values up to ten times larger than for the corresponding complexes of the "mixed" dipeptides. This type of preferential complexation of "pure" dipeptides can be explained by noting that the two nonpolar side chains of the "pure" dipeptide in $Cu(H_{-1}L)$ complexes are on the same side of the coordination plane, whereas they are on opposite sides in those of the "mixed" dipeptides. Hydrophobic bonding of the side chains with the amide group and with each other is suggested as the reason for the higher stability of the $Cu(H_{-1}L)$ complexes of the "pure" dipeptides. Hydroxo formation constants (K_{OH}) are the same for complexes of both "pure" and "mixed" dipeptides; this is expected because of the very similar structures of the $Cu(H_{-1}L)$ and $Cu(H_{-1}L)(OH)^-$ complexes.

The diverse functions of transition metal ions in biological systems depend in part upon the nature of the biological ligands which bind them. The particular importance of peptide binding to metal ions may be inferred from the large number of studies that have been carried out on metal–peptide complexes.[3,4] Yet little is known about metal ion binding of peptides having differing chiral centers. In the past, we examined the stereoselective binding of optically active amino acids by metal complexes bearing optically active ligands.[5] In this paper, we extend these studies to the stereoselective binding of optically active dipeptides by Cu(II) and Zn(II).

Metal ion binding of dipeptides (HL) in aqueous solution has been shown[3,4,6] to involve one or more of the following equilibria

$$M^{2+} + L^- \overset{K_1}{\rightleftharpoons} ML^+ \quad (1)$$

$$ML^+ + L^- \overset{K_2}{\rightleftharpoons} ML_2 \quad (2)$$

$$ML^+ \overset{K_{1a}}{\rightleftharpoons} M(H_{-1}L) + H^+ \quad (3)$$

Using optically active dipeptides, Li, *et al.*,[7] found that K_1 is larger for L,D-Ala-Ala (alanylalanine) than for L,L-Ala-Ala with Co(II). Likewise, K_1 was larger for D,L-Leu-Tyr (leucyltyrosine) than for L,L-Leu-Tyr with Co(II), Ni(II), and Zn(II). In contrast, Karczynski and Kupryszewski[8–10] found that the L,L diastereomers of both Leu-Tyr and Leu-Ala exhibited higher K_1 values than did their L,D isomers with Cu(II), Ni(II), and Zn(II). Since these authors were apparently unaware of the importance of the amide deprotonation equilibrium (eq 3) in the Cu(II) complexation reactions, it appears that their K_1 values are in error. After our studies were completed, a report by Kaneda (with A. E. Martell)[11] came to our attention. They found that K_1 values for the reaction of Cu(II) and Ni(II) with Ala-Ala and Leu-Tyr were larger for the L,D diastereomers than for the L,L derivatives. Values of K_{1a}, however, were larger for L,L dipeptides. Our interest in these equilibria was to examine the factors which give rise to the stereoselectivity of Cu(II) and Zn(II) in binding L,L and L,D dipeptides.

Experimental Section

Reagents. The D,L, D,D, and L,L isomers of leucylleucine (Leu-Leu) were purchased from Research Plus Laboratories, while the L,D isomer was purchased from Sigma Chemical Co. The L,L and

(1) Presented by R. N. at the 166th National Meeting of the American Chemical Society, Chicago, Ill., Aug 1973.
(2) Fellow of the Alfred P. Sloan Foundation, 1970–1972.
(3) H. C. Freeman in "Inorganic Biochemistry," G. L. Eichhorn, Ed., Elsevier, New York, N. Y., 1973, Chapter 4.
(4) E. Breslow, ref 3, Chapter 7.
(5) R. Nakon, P. R. Rechani, and R. J. Angelici, *Inorg. Chem.*, **12**, 2431 (1973), and references therein.
(6) M. K. Kim and A. E. Martell, *Biochemistry*, **3**, 1169 (1964).
(7) N. C. Li, G. W. Miller, N. Solony, and B. T. Gillis, *J. Amer. Chem. Soc.*, **82**, 3737 (1960).
(8) F. Karczynski and G. Kupryszewski, *Rocz. Chem.*, **41**, 1019 (1967).
(9) F. Karczynski and G. Kupryszewski, *Rocz. Chem.*, **41**, 1665 (1967).
(10) F. Karczynski and G. Kupryszewski, *Rocz. Chem.*, **43**, 1317 (1969).
(11) A. Kaneda, Ph.D. Dissertation, Texas A&M University, Jan 1973.